

Slow aggregation of lysozyme in alkaline pH monitored in real time employing the fluorescence anisotropy of covalently labelled dansyl probe

Lopamudra Homchaudhuri^a, Satish Kumar^b, Rajaram Swaminathan^{b,*}

^a Department of Chemistry, Indian Institute of Technology Guwahati, Guwahati 781 039, Assam, India

^b Department of Biotechnology, Indian Institute of Technology Guwahati, Guwahati 781 039, Assam, India

Received 19 January 2006; revised 3 March 2006; accepted 5 March 2006

Available online 10 March 2006

Edited by Christian Griesinger

Abstract The onset of hen egg white lysozyme aggregation on exposure to alkaline pH of 12.2 and subsequent slow growth of soluble lysozyme aggregates (at 298 K) was directly monitored by steady-state and time-resolved fluorescence anisotropy of covalently attached dansyl probe over a period of 24 h. The rotational correlation time accounting for tumbling of lysozyme in solution (40 μ M) increased from \sim 3.6 ns (in pH 7) to \sim 40 ns on exposure to pH 12.2 over a period of 6 h and remained stable thereafter. The growth of aggregates was strongly concentration dependent, irreversible after 60 min and inhibited by the presence of 0.9 M L-arginine in the medium. The day old aggregates were resistant to denaturation by 6 M guanidine \cdot HCl. Our results reveal slow segmental motion of the dansyl probe in day old aggregates in the absence of L-arginine (0.9 M), but a much faster motion in its presence, when growth of aggregates is halted. © 2006 Federation of European Biochemical Societies. Published by Elsevier B.V. All rights reserved.

Keywords: Lysozyme aggregation; Fluorescence anisotropy; Dansyl; Arginine

1. Introduction

Investigating the molecular basis of protein aggregation is important owing to its role in a number of neurodegenerative diseases like Alzheimer's and Parkinson's disease [1]. Recent findings indicate that soluble oligomers of proteins which are precursors in the pathway leading to insoluble amyloid fibrils are the toxic species [2–4]. Also, in most cases where protein aggregation and disease associated phenotypes were separated in time, fibrous proteinaceous inclusions were observed well after the onset of the behavioural or neuropathological symptoms [5]. Clearly, the soluble aggregates formed early in the aggregation pathway seem to play a major role in the neurodegenerative diseases.

Early diagnosis of amyloid disease has proved difficult because monitoring the early growth of protein aggregates has not been possible for two reasons: (i) a simple and sensitive method to specifically detect protein aggregates in solution is not available, and (ii) the rapid rate at which proteins aggregate in vitro (e.g., barstar, a ribonuclease inhibitor, aggregates almost instantaneously when transferred to pH 3 from pH 7 [6])

makes tracking difficult. A consequence of the latter is that, structural snapshots of the intervening steps of the aggregation pathway, which are important to develop a molecular level understanding, have remained inadequate. This report addresses both the above issues in protein aggregation. Once the method to monitor growth of aggregates was established, therapeutic strategies to inhibit the growth are easily tested and identified as shown by us in the case of L-arginine.

2. Materials and methods

2.1. Materials

Hen egg white lysozyme (HEWL) (L-6876) and L-arginine hydrochloride (A-5131) used in our studies was procured from Sigma–Aldrich Company Pvt. Ltd. 2-Dimethylaminonaphthalene-6-sulfonyl chloride (D-23), was obtained from Molecular Probes (Eugene, Oregon, USA).

2.2. Labelling with dansyl probe

For labelling, the procedure recommended by Molecular Probes was followed. To a 3 mM lysozyme solution in 1 ml of 0.1 M, pH 9 sodium bicarbonate buffer, 50 μ l of 75 mM dansyl chloride in DMF was added. The reaction mixture was kept at 4 °C with constant stirring for 3 h. Subsequently, 1.5 ml buffer was added to the reaction mixture. The unlabelled fluorophores were separated from the labelled protein solution using an Amersham PD-10 desalting column previously eluted with 50 mM, pH 7 sodium phosphate buffer. Protein and dye concentrations were determined by using absorbance at 280 and 339 nm, respectively. The molar extinction coefficient for the labelled probe at 339 nm is 3370 M^{−1} cm^{−1} [14,15]. The molar ratio of the protein to dye in the dye conjugated protein was calculated to be \sim 1:1. For aggregation experiments, stocks of the labelled protein in pH 7 buffer were diluted at least tenfold in 50 mM, pH 12.2 phosphate buffer.

2.3. Steady-state fluorescence

Steady-state fluorescence anisotropy measurements (*G* factor corrected) were made in Jobin-Yvon Fluoromax-3 spectrofluorometer equipped with automated Glan-Thompson polarisers and a PMT operating at a voltage of 950 V in photon counting mode. Slit widths for excitation at 370 nm were 1 nm and for emission at 444 nm between 5 and 10 nm. The background intensity from Raman scatter or buffer was negligible (<5%) compared to sample emission intensity under identical conditions as observed with blank samples.

2.4. Time-resolved fluorescence

Nanosecond time-resolved fluorescence intensity and anisotropy decay measurements were carried out in Fluorocube (IBH, Glasgow) using the time-correlated single photon counting method. The system was equipped with motorized Glan-Thompson polarisers and an IBH TBX04 photon-detection module. For excitation an IBH 370 nm NanoLED with a FWHM of 1.3 ns and a repetition rate of 1 MHz was used. Excitation light was attenuated, whenever required, using neutral density filters (OD = 3). A Schott UG-1 filter was also

*Corresponding author. Fax: +91 361 2690762.

E-mail address: rsw@iitg.ernet.in (R. Swaminathan).

used at the excitation end to cut out long wavelength glow from the 370 nm light source. Emission was detected after passing it through a Schott 420 nm long pass filter in order to block excitation photons. Fluorescence intensity decay was collected in 1024 channels, with a temporal resolution of 0.113 ns/channel. Peak counts were typically between 10 and 15 k. All measurements were done at 298 K.

The fluorescence intensity decay data were fit to a multi-exponential model using the IBH DAS6 fluorescence decay analysis software. The anisotropy decay data were fitted to multi-exponential decay model, as described earlier [6]. In both cases above, the goodness-of-fit was determined by reduced χ^2 and the randomness of the residuals. For anisotropy decay, the fits were additionally constrained to yield a calculated steady-state anisotropy value that is close to that observed independently using steady-state fluorimeter [6,17].

3. Results and discussion

Earlier reports using equilibrium sedimentation, have shown that HEWL (at 1 mM concentration) forms dimers in the pH range 5–9 and higher oligomers at pH 10–11 [8,9]. There are also reports on the formation of fibrils by hen egg white lysozyme at acidic pH and elevated temperatures [10,11]. Our results showed that the tendency to aggregate (at μM concentrations) was most pronounced at pH 12.2 (see [supplementary material](#)). Thus, exposure to alkaline pH of 12.2 served as a convenient approach to initiate the aggregation of HEWL.

Fluorescence anisotropy is an excellent technique to study the rotational motion of fluorophores in the excited state following their excitation using plane polarized light [7]. Steady-state fluorescence anisotropy (r_{ss}) gives us a time integrated average value of the rotational motion of molecules in the excited state. This parameter is however dependent both on the fluorescence lifetime and rotational correlation time of the fluorescent probe. Time-resolved anisotropy decay observations can reveal the multiple rotational motions experienced by the fluorophore in the excited state in terms of their rotational correlation time(s), ϕ_i . As ϕ arising from whole protein tumbling, is directly related to the size (volume) of the fluorophore conjugated protein from the Stokes–Einstein equation, any event, like protein aggregation, which changes the size of the protein can be directly monitored by measuring ϕ . In this work, HEWL was covalently tagged with the fluorescent probe, 2-dimethylaminonaphthalene-6-sulfonyl chloride (dansyl chloride from now on) in order to specifically monitor the rotational motion of lysozyme in solution under two different conditions: (a) pH 12.2 (aggregation prone condition); and (b) pH 7 (native state).

Fig. 1 shows the variation in fluorescence steady-state anisotropy (r_{ss}) of dansyl labelled lysozyme with time at pH 12.2 and pH 7 (control). At pH 7, no significant change in r_{ss} (~ 0.06) of lysozyme is observed for over a day, indicating that the overall structure of native protein is intact and unperturbed in this time span. At pH 12.2, immediately on exposure to alkaline pH, the r_{ss} increased to ~ 0.08 . Subsequently, we see a gradual increase in r_{ss} during the first 360 min, followed by saturation over a period of 24 h in contrast to pH 7 (native state). Importantly, the magnitude of this increase is dependent on the concentration of lysozyme from 4 to 200 μM (Fig. 1). At 4 μM , the r_{ss} saturates at 0.13, while with 40 μM it settles down at 0.15 and finally at 200 μM , it stabilises at 0.20. Time-resolved fluorescence intensity decays with 40 μM lysozyme have revealed the following: (a) the mean fluorescence

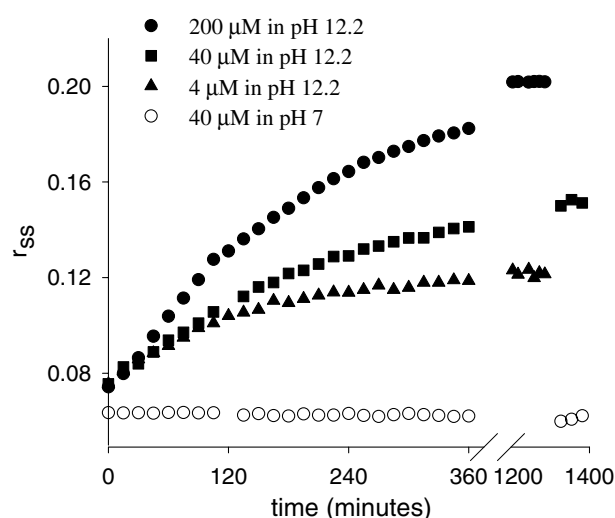


Fig. 1. Change in steady-state anisotropy of dansyl labelled lysozyme with time. pH 7, 40 μM , open circles; pH 12.2, 4 μM , filled triangles; pH 12.2, 40 μM , filled squares; and pH 12.2, 200 μM (only 40 μM was dansyl labelled, rest are unlabelled), filled circles. All measurements were done at 298 K.

lifetime of dansyl conjugated HEWL (Fig. 2) was constant over the period of first 360 min shown in Fig. 1, and (b) the mean fluorescence lifetime at pH 12.2 showed no significant variation compared to that at pH 7 (Fig. 2). Therefore, the quantum yield of the dansyl probe is fairly constant with time and unaffected by change in pH. Covalent linkage of the dansyl chromophore to a solvent exposed lysine residue on the surface can account for this insensitivity of dansyl quantum yield to lysozyme aggregation. Therefore, the observed increase in r_{ss} at pH 12.2, can only occur owing to a large increase in average rotational correlation time of dansyl probe. This would

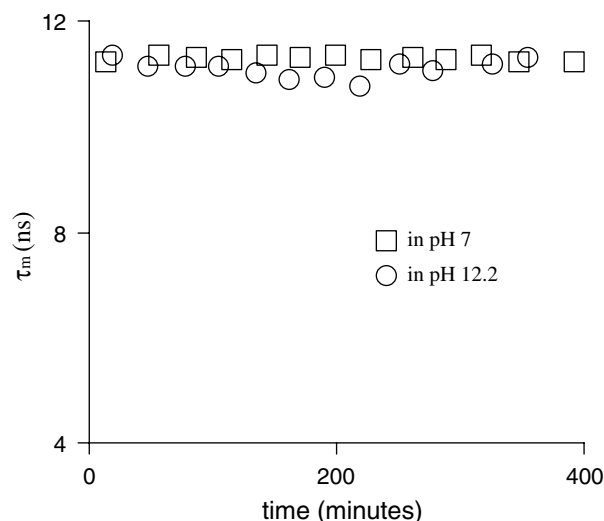


Fig. 2. The mean fluorescence lifetime, τ_m , of 40 μM dansyl labelled lysozyme was calculated using the formula $\tau_m = \sum_{i=1}^3 \alpha_i \tau_i$, where τ_i and α_i correspond to the i th lifetime component and its amplitude, respectively. The intensity decays (see [supplementary material](#)) were monitored over a period of ~ 360 min. The mean fluorescence lifetimes (τ_m) were determined in pH 7 (open squares) and in pH 12.2 buffer (open circles).

imply an increase in the size of lysozyme with time. The concentration dependence of the rise in r_{ss} is a clear indicator of the formation of higher oligomers, since the growth kinetics would depend on the concentration of monomers. Apparently, higher protein concentrations favour aggregates of larger size as evident from Fig. 1. It must be noted that the 200 μ M sample contained only 40 μ M of labelled lysozyme. This implies that labelled and unlabelled lysozyme are not differentiated during aggregation. Importantly, it also indicates that dansyl group had no role in promoting aggregation. Another striking feature in the progress of this aggregation is the absence of a lag phase. More investigations at faster time scales (s or ms) are however required to probe this. It must be borne in mind that as r_{ss} does not yield the population of aggregated species, thus it cannot be used to estimate the kinetic constants. In order to confirm the observations in Fig. 1, time-resolved fluorescence anisotropy measurements were carried out.

Fig. 3 shows anisotropy decay profiles of the 40 μ M labelled-lysozyme at pH 7 and pH 12.2 (at different time points). The values of the fitted parameters are shown in Table 1 (see supplementary material for the fits with residuals). At pH 7, the anisotropy showed a monoexponential decrease to zero with time, yielding a rotational correlation time (ϕ) of 3.6 ns. No major change was observed in ϕ over a period of 24 h. A value of 3.6 ns for native lysozyme is consistent with a previous reported value (3.8 ns) [12]. Note that r_0 (and calculated r_{ss}) is less at pH 7, owing to fast segmental motion in the subnanosecond scale which cannot be detected in our instrument owing to excitation pulse width ~ 1.3 ns (fwhm). At pH 12.2, unlike pH 7, starting with $t = 15$ min a finite residual anisotropy (r_{∞}) is evident at longer time (~ 30 ns). The r_{∞} , shows a gradual increase with time till $t = 355$ min. A minor drop in r_{∞} occurs after overnight incubation. The slow ~ 9.6 ns component observed initially might arise from an oligomer. The short correlation time (~ 2.4 ns) arises from fast segmental motion, most likely about the long lysine side chain. At $t = 60$ min, the anisotropy decay did not yield a good fit (reduced $\chi^2 = 3.1$) for two-exponential model. A three-exponential fit (reduced $\chi^2 = 1.4$) revealed, rotational correlation times, 1.4, 7.0 and 42 ns with amplitudes 0.19, 0.52 and 0.29, respectively. This indicates a heterogeneous ground state ensemble population

in the transitional phase, owing to a mixture of dimeric/trimeric and large multimeric aggregates. As time progresses, the 7–9.6 ns component seems to get transformed to ~ 40 ns, yielding a better biexponential fit. This represents a clear increase in population of larger aggregates. After 200 min, we observe that the long component has stabilised to a constant amplitude (population). A 39–45 ns rotational correlation time would imply a multimeric lysozyme aggregate. Overnight incubation does not affect the size of the aggregate significantly (Table 1). In fact, no appreciable change was observed after several days either. The change in the short component from 2.4–1.4 initially to 3.5–4.1 ns much later is interesting. It reveals that segmental motion of the dansyl probe is relatively free when HEWL is in the form of smaller aggregates (oligomers) early on, but becomes more hindered as larger multimeric aggregates begin to dominate. The aggregated protein clearly does not provide sufficient freedom for segmental motion. Table 1 also shows that a significant fraction ($>60\%$) of

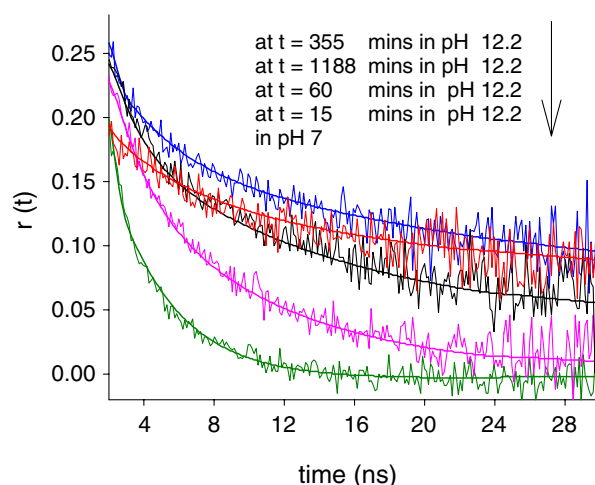


Fig. 3. Time-resolved anisotropy decay of dansyl labelled lysozyme (40 μ M) under different conditions. Dark green, pH 7; magenta, pH 12.2 after 15 min; black, pH 12.2 after 60 min; red, pH 12.2 after 1188 min; and blue pH 12.2 after 355 min. See Table 1 for details on the fitted curves.

Table 1
Details of fits to anisotropy decay curves in Figs. 3 and 4

pH	t (min)	r_0^a	r_{ss}^b	ϕ_1^c (ns)	ϕ_2^c (ns)	ϕ_3^c (ns)	α_1^d	α_2^d	α_3^d	χ^2_{re}
7.0	—	0.18	0.04	3.6	—	—	1.0	—	—	1.6
12.2	15	0.24	0.08	2.4	9.6	—	0.40	0.60	—	1.4
12.2	60	0.26	0.12	1.4	7.0	42	0.19	0.52	0.29	1.4
12.2	100	0.23	0.13	5.3	39	—	0.53	0.47	—	1.4
12.2	215	0.24	0.14	3.7	39	—	0.36	0.64	—	1.4
12.2	355	0.25	0.15	4.1	45	—	0.36	0.64	—	1.5
12.2	1188	0.22	0.14	3.5	43	—	0.32	0.68	—	1.6
12.2, 0.9 M Arg	22	0.25	0.11	2.9	14	—	0.33	0.67	—	1.4
12.2, 0.9 M Arg	60	0.23	0.11	2.5	18	—	0.29	0.71	—	1.4
12.2, 0.9 M Arg	135	0.23	0.11	3.3	20	—	0.37	0.63	—	1.4
12.2, 0.9 M Arg	300	0.23	0.11	2.6	17	—	0.33	0.67	—	1.5
12.2, 0.9 M Arg	1140	0.20	0.07	1.9	13	—	0.49	0.51	—	1.6

The errors in the values reported for ϕ_1 are within 10%, while those for ϕ_2 and ϕ_3 are within 5%, based on results from multiple experiments.

^aInitial anisotropy.

^bSteady-state anisotropy calculated from fit.

^cRotational correlation time(s).

^dFractional amplitudes associated with correlation time.

^eReduced χ^2 for the fit.

the anisotropy decay in the aggregated protein is accounted by tumbling of the whole protein. This feature of dansyl-labelled HEWL makes it easy to track aggregation by simpler methods like steady-state anisotropy as shown in Fig. 1. Taken together, the data clearly support the growth of lysozyme aggregates with time and their subsequent stability. Unlike a previous report [16], which used fluorescein (lifetime = 4 ns) our use of a long lifetime dansyl probe (lifetime = 11 ns) permits unambiguous measurement of the size of aggregates in terms of their rotational correlation time.

There have been earlier reports of arginine being effective in suppressing the aggregation of denatured lysozyme [13, and references cited therein], but nature of lysozyme aggregate(s) in the presence of arginine remains to be defined. We have investigated the effect of L-arginine on the aggregation of the labelled lysozyme in pH 12.2 buffer. We employed 0.9 M L-arginine hydrochloride in our studies with the intention to bring a marked influence on aggregation, based on reports from previous work [13], where L-arginine concentrations up to 1 M have been employed. From Fig. 4 and Table 1, it is clear that in the presence of arginine, the longer correlation time initially shows a higher value, ~14 ns. This may occur due to a minor increase in bulk viscosity (~1.5-fold as measured by a viscometer) in the presence of 0.9 M arginine. Thus the observed ~14 ns component is actually the ~9.6 ns component observed in the absence of arginine. This value gradually increases to 20 ns later at 135 min suggesting a minor progress in aggregation. After overnight incubation in the presence arginine, the longer component stabilised around ~13 ns, which is similar to the size which we observed initially ($t = 22$ min). The larger aggregate (~20 ns component) has clearly broken down into smaller oligomers. The ~13–14 ns component, like the ~9.6 ns component, is likely to arise from a small oligomer of lysozyme. Control experiments in the absence of arginine, done simultaneously under identical conditions, revealed a long correlation time ~42 ns consistent with previous results. It is apparent that the presence of arginine is effective in arresting the growth of aggregates. The presence of arginine clearly prevents the formation of large aggregates (~40 ns component). Interestingly, the short component (~1.9 ns) at

1140 min in the presence of 0.9 M arginine (1.5-fold more viscous), reveals a much faster segmental motion (compared to ~3.5 ns in aggregates in the absence of arginine) with a significantly higher amplitude (~0.49). A lower value of initial anisotropy (r_0) is also a proof of this. Obviously, rotation of the dansyl probe about lysine side chain in small oligomers in the prolonged presence of arginine is much less hindered suggesting a loosely packed protein.

Previous work [13] has suggested that L-arginine increases the equilibrium solubility of the denatured state(s) of lysozyme by stabilising these state(s) against pathways such as aggregation by most likely acting as hydrogen bond donors. Another recent work [18] has suggested that arginine inhibits aggregation by slowing protein–protein association reactions by being preferentially excluded from protein–protein encounter complexes, but not from dissociated protein monomers. Our results here reveal two competing, but opposite pathways in the presence of 0.9 M L-arginine. One weakly favouring aggregation (in comparison to aggregation tendency in the absence of arginine) and the other strongly opposing aggregation, but favoring a more unfolded protein. Initially the weak aggregation pathway seems to have a lead, as observed by small, but gradual increase in rotational correlation time for global motion (~20 ns at 135 min, amplitude = 0.63) and segmental motion (3.3 ns at 135 min, amplitude = 0.37). Later, the pathway opposing aggregation takes over and begins to dominate (see Table 1). After an overnight incubation at room temperature, a relative decrease in the magnitude of rotational correlation time for both segmental motion (1.9 ns at 1140 min, amplitude = 0.49) and global tumbling (13 ns at 1140 min, amplitude = 0.51) accompanied by a relative increase in amplitude of fast segmental motion is evident compared to earlier times. This argues in favour of a relatively more unfolded, small oligomer of lysozyme compared to that in the absence of arginine. This unfolded state is stabilised by the presence of L-arginine and resists aggregation consistent with earlier reports [13,18]. Clearly an equilibration time of about a day is required to fully realise the inhibitory influence of arginine on protein aggregation. It would be worthwhile to explore the kinetics of aggregation inhibition with different derivatives of L-arginine to obtain clues on the mechanism of inhibition. This work is in progress.

We investigated the reversibility of the oligomers formed. For this, we transferred aliquots of aggregates [40 μ M] at different time points in Fig. 1 to pH 7 (100 mM phosphate) and measured the steady-state anisotropy immediately after dilution and after overnight incubation (see supplementary material). A marginal decrease was observed in pH 7 at early times (~30 min), while later (~60 min) the r_{ss} values were similar to that observed with alkaline pH, indicating that the oligomerization that occurs at pH 12.2 is irreversible after the initial 60 min. Interestingly, the appearance of the long component (~42 ns) also becomes apparent from ~60 min onwards (see Table 1 and earlier discussion). Thus, the onset of irreversibility is clearly linked to the formation of larger aggregates. Earlier studies, have revealed that HEWL (at 1 mM concentration) polymerizes reversibly with increasing pH, studied up to pH 11 [8,9].

We attempted to denature the day old lysozyme aggregates (40 μ M) by transferring them (1:10 dilution) to a solution containing 6 M guanidine · HCl at pH 7. The r_{ss} immediately after transfer was 0.128 ± 0.002 , and while it was 0.117 ± 0.001 after

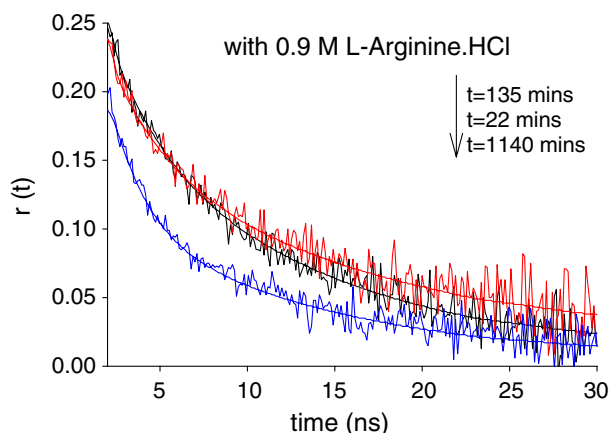


Fig. 4. Time-resolved anisotropy decay of dansyl labelled lysozyme (40 μ M) at pH 12.2 in the presence of 0.9 M arginine is shown for different time intervals subsequent to exposure to alkaline pH. Black curve, $t = 22$ min, red curve $t = 135$ min and blue curve, $t = 1140$ min. See Table 1 for details on the fitted curves.

overnight incubation at 298 K in the same medium. The aggregates formed are clearly resistant to denaturation.

In order to confirm that the observed aggregation is not due to covalent modification of the amino group, studies were carried out with unlabelled lysozyme. It is worthwhile to recall here that in Fig. 1, the steady-state anisotropy observed at pH 12.2 with 200 μ M lysozyme sample, contained 160 μ M of unlabelled lysozyme. In addition, the formation of aggregates in unlabelled lysozyme (150 μ M, pH 12.2) was clearly observed from the rise in light scattering ($\lambda = 350$ nm) intensity using vertically polarised light in the spectrofluorometer in contrast to lysozyme (150 μ M) at pH 7 (see supplementary material). Hence, it is unlikely that aggregation is promoted by the covalent modification of lysozyme.

In conclusion, we show that soluble aggregates in the early stages of protein aggregation can be unambiguously tracked in real time using fluorescence anisotropy of labelled dansyl probe. Our data reveal that segmental motion is hindered in aggregated protein. In the presence of 0.9 M arginine when the progress of aggregation is arrested, we show that segmental motion is quite free, while the protein itself is likely to be loosely packed. We also show that irreversibility of aggregation is likely to coincide with the appearance of large multi-meric aggregates. Finally, the slow aggregation kinetics of lysozyme in alkaline pH can perhaps provide an experimental model to understand the molecular events during aggregation in structural detail given the wealth of structural data available in PDB for this well characterised protein.

Acknowledgements: We thank Prof. N. Periasamy for the anisotropy decay analysis software and Prof. G. Krishnamoorthy for discussions. We are thankful to Indian Institute of Technology Guwahati for providing the experimental facilities.

Appendix A. Supplementary data

Supplementary data associated with this article can be found, in the online version, at [doi:10.1016/j.febslet.2006.03.012](https://doi.org/10.1016/j.febslet.2006.03.012).

References

- [1] Thirumalai, D., Klimov, D.K. and Dima, R.I. (2003) Emerging ideas on the molecular basis of protein and peptide aggregation. *Curr. Opin. Struct. Biol.* 13, 146–159.
- [2] Walsh, D.M., Klyubin, I., Fadeeva, J.V., Cullen, W.K., Anwyl, R., Wolfe, M.S., Rowan, M.J. and Selkoe, D.J. (2002) Naturally secreted oligomers of amyloid beta protein potently inhibit hippocampal long term potentiation *in vivo*. *Nature* 416, 535–539.
- [3] Bucciantini, M., Giannoni, E., Chiti, F., Baroni, F., Formigli, L., Zurdo, J., Taddei, N., Ramponi, G., Dobson, C.M. and Stefani, M. (2002) Inherent toxicity of aggregates implies a common mechanism for misfolding diseases. *Nature* 416, 507–511.
- [4] Lambert, M.P., Barlow, A.K., Chromy, B.A., Edwards, C., Freed, R., Liosatos, M., Morgan, T.E., Rozovsky, I., Trommer, B. and Viola, K.L. (1998) Diffusible, nonfibrillar ligands from Abeta 1–42 are potent central nervous system neurotoxins. *Proc. Natl. Acad. Sci. USA* 95, 6448–6453.
- [5] Caughey, B. and Lansbury Jr., P.T. (2003) Protofibrils, pores, fibrils and neurodegeneration: Separating the responsible protein aggregates from the innocent bystanders. *Annu. Rev. Neurosci.* 26, 267–298.
- [6] Swaminathan, R., Periasamy, N., Udgaonkar, J.B. and Krishnamoorthy, G. (1994) Molten globule like conformation of barstar: a study by fluorescence dynamics. *J. Phys. Chem.* 98, 9270–9278.
- [7] Lakowicz, J.R. (1999) *Principles of Fluorescence Spectroscopy*, Kluwer Academic/Plenum Press, New York.
- [8] Sophianopoulos, A.J. and van Holde, K.E. (1961) Evidence for dimerization of lysozyme in alkaline solution. *J. Biol. Chem.* 236, PC82–PC83.
- [9] Sophianopoulos, A.J. and van Holde, K.E. (1964) Physical studies of muramidase (lysozyme): pH dependent dimerization. *J. Biol. Chem.* 239, 2516–2524.
- [10] Arnaudov, L.N. and de Vries, R. (2005) Thermally induced fibrillar aggregation of hen egg white lysozyme. *Biophys. J.* 88, 515–526.
- [11] Krebs, M.R.H., Wilkins, D.K., Chung, E.W., Pitkeathly, M.C., Chamberlain, A.K., Zurdo, J., Robinson, C.V. and Dobson, C.M. (2000) Formation and seeding of amyloid fibrils from wild-type hen lysozyme and a peptide fragment from the beta domain. *J. Mol. Biol.* 300, 541–549.
- [12] Vos, K., van Hoek, A. and Visser, A.J. (1987) Application of a reference convolution method to tryptophan fluorescence in proteins. A refined description of rotational dynamics. *Eur. J. Biochem.* 165, 55–63.
- [13] Reddy, R.C.K., Lilie, H., Rudolph, R. and Lange, C. (2005) L-Arginine increases the solubility of unfolded species of hen egg white lysozyme. *Protein Sci.* 14, 929–935.
- [14] Levi, V. and Flecha, F.L.G. (2003) Labeling of proteins with fluorescent probes. Photophysical characterization of dansylated bovine serum albumin. *Biochem. Mol. Biol. Educ.* 31, 333–336.
- [15] Chen, R.F. (1968) Dansyl labeled proteins: determination of extinction coefficient and number of bound residues with radioactive dansyl chloride. *Anal. Biochem.* 25, 412–416.
- [16] Allsop, D., Swanson, L., Moore, S., Davies, Y., York, A., El-Agnaf, O.M.A. and Soutar, I. (2001) Fluorescence anisotropy: a method for early detection of Alzheimer beta-peptide(A β) aggregation. *Biochem. Biophys. Res. Commun.* 285, 58–63.
- [17] Feinstein, E., Deikus, G., Rusinova, E., Rachofsky, E.L., Ross, J.B.A. and Laws, W.R. (2003) Constrained analysis of fluorescence anisotropy decay: application to experimental protein dynamics. *Biophys. J.* 84, 599–611.
- [18] Baynes, B.M., Wang, D.I.C. and Trout, B.L. (2005) Role of arginine in stabilisation of proteins against aggregation. *Biochemistry* 44, 4919–4925.